

# Enhanced emission efficiency of GaN/InGaN multiple quantum well light-emitting diode with an embedded photonic crystal

Min-Ki Kwon,<sup>1</sup> Ja-Yeon Kim,<sup>1</sup> Il-Kyu Park,<sup>1</sup> Ki Seok Kim,<sup>1</sup> Gun-Young Jung,<sup>1</sup> Seong-Ju Park,<sup>1(a)</sup> Je Won Kim,<sup>2</sup> and Yong Chun Kim<sup>2</sup>

<sup>1</sup>Department of Materials Science and Engineering, Gwangju Institute of Science and Technology (GIST), Gwangju 500-712, Republic of Korea

<sup>2</sup>Samsung Electro-Mechanics, Suwon 443-743, Republic of Korea

(Received 13 March 2008; accepted 28 May 2008; published online 26 June 2008)

A photonic crystal (PC) structure of periodic SiO<sub>2</sub> pillar cubic array is embedded in *n*-GaN layer of InGaN/GaN multiple quantum well (MQW) blue (480 nm) light-emitting diode (LED). The diameter, period, and depth of SiO<sub>2</sub> pillar are 124 ± 6, 230 ± 10, and 130 ± 10 nm, respectively. The increments of 70% for external quantum efficiency, 17% for internal quantum efficiency, and 45% for light extraction efficiency from photoluminescence measurement, and 33% for optical output power at 20 mA are observed for LEDs with an embedded PC layer. This improvement can be attributed to the increased extraction efficiency by PC effect as well as increased internal quantum efficiency due to the decrease of dislocation density in *n*-GaN layer because of an epitaxial lateral over-growth process. © 2008 American Institute of Physics. [DOI: 10.1063/1.2948851]

Highly efficient GaN-based light-emitting diodes (LEDs) have been intensively developed in recent years for various applications, such as traffic lights, full color displays, liquid crystal display back lightings, and solid-state lighting. This widespread application makes it desirable to increase the internal quantum efficiency ( $\eta_{\text{int}}$ ) and light extraction efficiency ( $\eta_{\text{extraction}}$ ) of LEDs.<sup>1</sup> Recent crystal growth technology has improved the  $\eta_{\text{int}}$ , while  $\eta_{\text{extraction}}$  still remains low because of total internal reflection at the surfaces of the LEDs due to the difference in refractive index between GaN ( $n=2.5$ ) and air ( $n=1$ ). To enhance  $\eta_{\text{extraction}}$ , various methods such as the metal reflection layer,<sup>2</sup> omnidirectional reflector,<sup>3</sup> textured surface,<sup>4-6</sup> and triangular chip design<sup>7</sup> have been considered. In addition, photonic crystal (PC) structures, which are materials with a spatially periodic refractive index, have also been investigated to improve the  $\eta_{\text{extraction}}$ .<sup>8-15</sup> LEDs containing PC structure have been designed to efficiently couple light from the guided modes into air.<sup>8,9</sup>

Until now, two-dimensional (2D) PC structures for enhancement of  $\eta_{\text{extraction}}$  in III-nitride based LED have generally been formed directly in the *p*-GaN layer.<sup>10-14</sup> Forming a PC structure in the *p*-GaN layer requires the use of plasma dry etching, resulting in plasma damage to the *p*-GaN layer and sometimes even in the multiple quantum well (MQW) layer. Many groups have reported that the electrical characteristics of LEDs containing etched PC structures were degraded due to etching damage to the *p*-GaN and reduction of the effective ohmic contact area due to 2D etched hole array.<sup>10-12,14</sup> In addition, the optimum thickness for a PC structure is known to be on the order of half the wavelength.<sup>15</sup> The thickness of the *p*-GaN layer, however, is generally limited to ~0.2 μm due to the poor crystal quality of *p*-GaN, Mg diffusion into the MQW layer, and thermal damage to the MQW layer at growth temperature higher than that for MQW.<sup>16,17</sup> Therefore, the PC structure formed in the

*p*-GaN layer is generally thinner than the thickness of *p*-GaN.

To solve the problems of electrical deterioration and thickness limitation of PC layer in PC LEDs, we propose a method of embedding the PC structure in the *n*-GaN using SiO<sub>2</sub> and GaN with different refractive indices. The  $\eta_{\text{extraction}}$  of LED with the embedded PC was markedly enhanced by PC effect without degradation of the electrical properties.

The InGaN/GaN MQW LEDs with an embedded PC structure were grown on a (0001) sapphire substrate by metal-organic chemical vapor deposition (MOCVD). The substrates were initially treated in H<sub>2</sub> at 1020 °C, followed by the growth of a 25-nm-thick low temperature GaN buffer layer at 550 °C. After high temperature annealing of the buffer layer, a 2-μm-thick *n*-GaN layer were deposited at a temperature of 1020 °C. Figure 1 illustrates the process flow

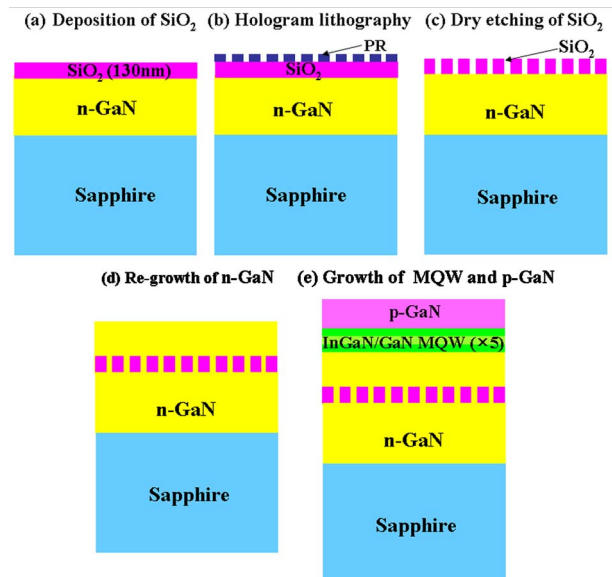


FIG. 1. (Color online) A schematic of the fabrication process for LED with an embedded PC.

<sup>a)</sup> Author to whom all correspondence should be addressed. Electronic mail: sjpark@gist.ac.kr.

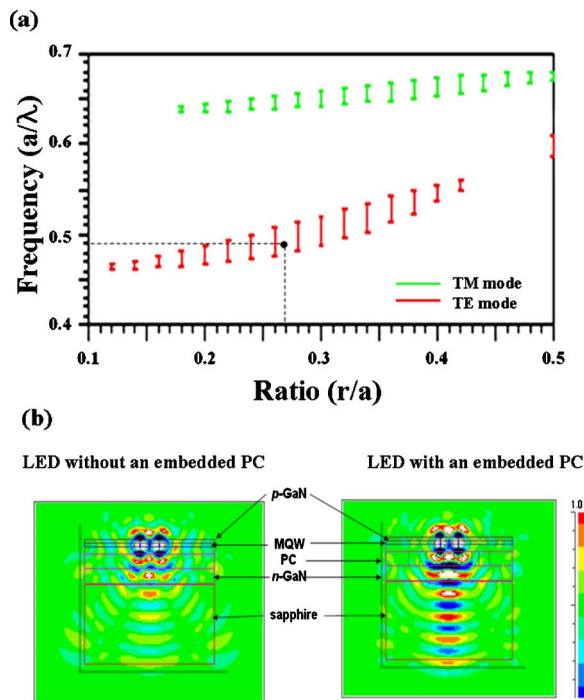


FIG. 2. (Color online) (a) The gap map for embedded PC with a cubic lattice array of  $\text{SiO}_2$  pillars surrounded by GaN and (b) 3D-FDTD simulation of light propagation in LEDs with and without an embedded PC.

to show the fabrication process for LED with the embedded PC consisting of  $\text{SiO}_2$  pillars and  $n$ -GaIn layers. For a comparative study, we also grew LED without an embedded PC on the same  $n$ -GaIn template using the same growth condition. A detailed procedure for the fabrication of LEDs with a size of  $300 \times 300 \mu\text{m}^2$  has been published elsewhere.<sup>2</sup>

The embedded PC structure was designed using a simulation program based on the preconditioned conjugate-gradient plane-wave expansion method.<sup>8,9</sup> Figure 2(a) depicts the normalized frequency ( $\omega a/2\pi c = a/\lambda$ ) as a function of the ratio ( $r/a$ ) for a PC structure consisting of a cubic array of 130-nm-thick  $\text{SiO}_2$  pillars surrounded by GaN. Figure 2(a) also shows the band gaps for the transverse-electric (TE) and transverse-magnetic (TM) modes. This study is focused on TE guided mode bands which are characterized by light propagating in parallel to the slab of LED (Ref. 8) since it is reported that TE polarization dominates in the InGaIn/GaN MQW LEDs.<sup>18</sup> For an optimum 2D-PC structure in blue LEDs, a frequency ( $a/\lambda$ ) of 0.49 and ratio ( $r/a$ ) of 0.27 were used for the blue light ( $\lambda = 480 \text{ nm}$ ), as illustrated in Fig. 2(a). Based on this information, the optimum diameter and period of the  $\text{SiO}_2$  pillars were estimated to be 127 and 230.4 nm, respectively. To predict the light extraction efficiency and the propagation of light emitted from the MQW via the PC structure, we employed the three-dimensional finite difference time domain (3D-FDTD) simulation based on a genetic algorithm with periodic boundary condition introduced by the 2D cubic array of the pillar structure.<sup>19</sup> Figure 2(b) contains the result of FDTD simulation of a blue LED with and without an embedded PC. Figure 2(b) clearly shows that the light emitted from the MQW structure of an LED with the embedded PC propagates more vertically, compared to an LED without an embedded PC. This can be attributed to the enhanced  $\eta_{\text{extraction}}$  in the vertical direction of LED because the embedded PC generates a

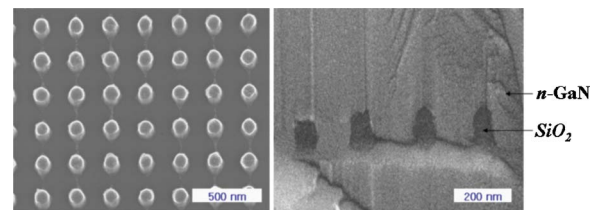


FIG. 3. (Color online) SEM images of (a) top view of  $\text{SiO}_2$  pattern and (b) side view of an embedded PC of  $\text{SiO}_2$  pillars surrounded by GaN.

photonic band gap (PBG) where photons with frequencies within the PBG are not allowed to propagate.<sup>14</sup> By employing a method for FDTD simulation published in Ref. 18, the  $\eta_{\text{extraction}}$  of blue LED with an embedded PC was estimated to be increased by a factor of 2, compared to that of blue LED without the embedded PC.

Figure 3(a) shows the scanning electron microscope (SEM) images of  $\text{SiO}_2$  pillars etched by RIE plasma through a laser hologram patterned photoresist mask. The diameter, period, and height of the  $\text{SiO}_2$  pillars are  $124 \pm 6$ ,  $230 \pm 10$ ,  $130 \pm 10 \text{ nm}$ , respectively. Figure 3(b) depicts the SEM images of cross-sectional view of the  $n$ -GaIn layer laterally reovergrown over the  $\text{SiO}_2$  pillars pattern by epitaxial lateral overgrowth (ELOG) process, showing that the  $\text{SiO}_2$  pillars are surrounded by the GaIn layer.

To measure the performance of the embedded PC, the MQW layer was photoexcited through the  $p$ -GaIn layer using He-Cd laser. The photoluminescence (PL) emission was measured from the bottom side of the sapphire substrate using a photodiode as indicated in the inset of Fig. 4(a). Figure 4(a) shows the room temperature PL spectra of MQW in LEDs with and without an embedded PC. The integrated intensity of the PL peak at 480 nm of MQW with an embedded PC was increased by 70%, compared to that of MQW

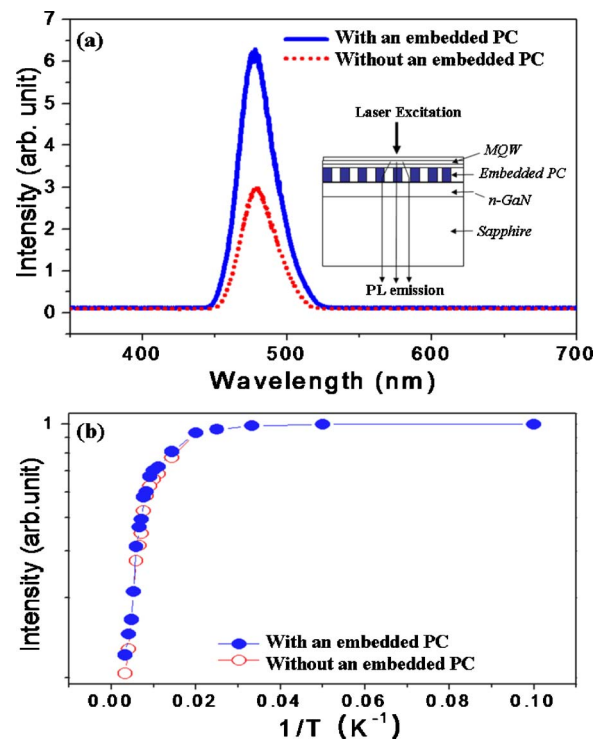


FIG. 4. (Color online) (a) Room temperature PL spectra of blue LED with and without an embedded PC and (b) temperature dependent integrated PL intensity of LED with and without an embedded PC.

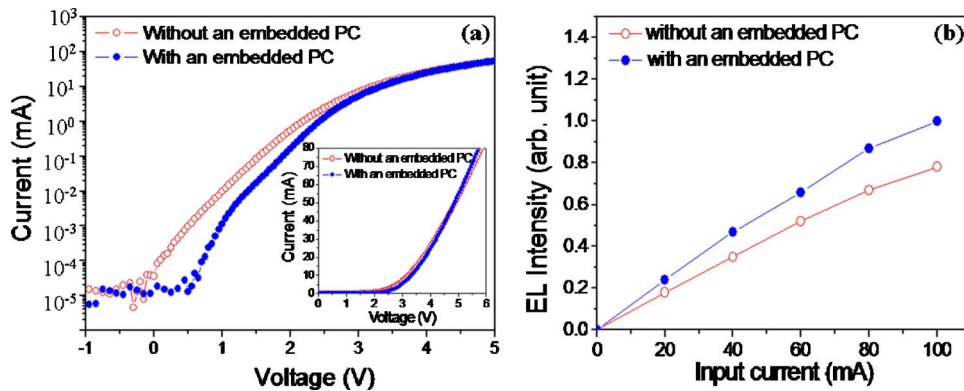


FIG. 5. (Color online) (a)  $I$ - $V$  characteristic and (b) optical output power ( $L$ - $I$ ) of blue LED with and without an embedded PC.

without an embedded PC. The increased PL intensity indicates an improvement in the external quantum efficiency ( $\eta_{\text{ext}}$ ) of MQW with an embedded PC, which is a product of  $\eta_{\text{int}}$  and  $\eta_{\text{extraction}}$ .

$$\eta_{\text{ext}} = \eta_{\text{int}} \times \eta_{\text{extraction}} \quad (1)$$

To investigate the enhancement of the  $\eta_{\text{int}}$  and  $\eta_{\text{extraction}}$  in LED with an embedded PC, we measured the temperature dependent PL spectra at temperatures ranging from 10 to 300 K as shown in Fig. 4(b). The  $\eta_{\text{int}}$  of InGaN/GaN MQWs was estimated by comparing PL intensities assuming that the  $\eta_{\text{int}}$  is 100% at low temperature (10 K) regardless of excitation carrier density.<sup>19</sup> As Fig. 4(b) shows, the  $\eta_{\text{int}}$  of MQW with and without an embedded PC at 300 K was 14.5% and 11.5%, respectively, indicating that the  $\eta_{\text{int}}$  of MQW was increased by 17% due to the embedded PC structures. The increase in  $\eta_{\text{int}}$  with an embedded PC can be attributed to reduction of defects such as screw and edge-type threading dislocations in the  $n$ -GaN and MQW layer. The growth mechanism of  $n$ -GaN is very similar to the ELOG GaN growth process, where SiO<sub>2</sub> pattern is used as a mask.<sup>20</sup> Based on the observed increases of 70% for  $\eta_{\text{ext}}$  and 17% for  $\eta_{\text{int}}$ , the increase in  $\eta_{\text{extraction}}$  was estimated to be 45% from Eq. (1) for LED with an embedded PC. The increase of 45% in  $\eta_{\text{extraction}}$  is attributed to the enhanced light extraction from LED by the embedded PC.

Figures 5(a) and 5(b) represent the current-voltage ( $I$ - $V$ ) characteristics and optical output power of LEDs with and without an embedded PC. The forward voltage of LED with and without an embedded PC is nearly same as shown in the inset of Fig. 5(a). However, the forward leakage current of LED with an embedded PC was decreased compared to that of LED without an embedded PC, as shown in Fig. 5(a). This reduction of forward leakage current is believed to be due to the decrease in dislocation density in LED.<sup>20</sup> The optical output power of LED with an embedded PC structure was increased by 33% compared to that of LED without embedded PC at an input current of 20 mA as shown in Fig. 5(b). This improvement in the optical output power of LED is most likely due to the increase in the  $\eta_{\text{extraction}}$  by the PC effect and improvement of the  $\eta_{\text{int}}$  resulting from a decrease in dislocation density. To further improve the efficiency of LED with embedded PC, it is necessary to optimize the thickness of the SiO<sub>2</sub> pillars.

In summary, we have investigated the effect of the embedded PC on  $\eta_{\text{ext}}$  of blue LED. The embedded PC markedly improved the PL and the optical output power of LED. The

improvement in optical and electrical properties were attributed to the increase of  $\eta_{\text{extraction}}$  by the embedded PC and  $\eta_{\text{int}}$  due to a reduction in dislocation density as a results of ELOG growth of  $n$ -GaN layer.

This work was supported by wide bandgap optoelectronic device research laboratory of the Korea Science and Engineering Foundation (KOSEF) grant funded by the Korea government (MOST) (No. R17-2007-078-01000-0), BK 21 program and Samsung Electro-Mechanics Co., Ltd. in Korea.

- <sup>1</sup>E. F. Schubert, *Light-Emitting Diode* (Cambridge University Press, New York, 2006).
- <sup>2</sup>J. Y. Kim, S. I. Na, G. Y. Ha, M. K. Kwon, I. K. Park, J. H. Lim, S. J. Park, M. H. Kim, D. Choi, and K. Min, *Appl. Phys. Lett.* **88**, 043507 (2006).
- <sup>3</sup>J. K. Kim, T. Gessmann, H. Luo, and E. F. Schubert, *Appl. Phys. Lett.* **84**, 4508 (2004).
- <sup>4</sup>C. Huh, K. S. Lee, E. J. Kang, and S. J. Park, *J. Appl. Phys.* **93**, 9383 (2003).
- <sup>5</sup>S. I. Na, G. Y. Ha, D. S. Han, S. S. Kim, J. Y. Kim, J. H. Lim, D. J. Kim, K. I. Min, and S. J. Park, *IEEE Photonics Technol. Lett.* **18**, 1512 (2006).
- <sup>6</sup>I. Schnitzer, E. Yablonovitch, C. Caneau, T. J. Gmitter, and A. Scherer, *Appl. Phys. Lett.* **63**, 2174 (1993).
- <sup>7</sup>J. Y. Kim, M. K. Kwon, J. P. Kim, and S. J. Park, *IEEE Photonics Technol. Lett.* **19**, 1865 (2007).
- <sup>8</sup>S. Fan, P. R. Villeneuve, J. D. Joannopoulos, and E. F. Schubert, *Phys. Rev. Lett.* **78**, 3294 (1997).
- <sup>9</sup>E. Yablonovitch, T. J. Gmitter, and R. Bhat, *Phys. Rev. Lett.* **61**, 2546 (1987).
- <sup>10</sup>T. N. Oder, H. S. Kim, J. Y. Lin, and H. X. Jiang, *Appl. Phys. Lett.* **84**, 466 (2004).
- <sup>11</sup>J. Shakyia, K. H. Kim, J. Y. Lin, and H. X. Jiang, *Appl. Phys. Lett.* **85**, 142 (2004).
- <sup>12</sup>D. H. Kim, C. O. Cho, Y. G. Roh, H. Jeon, Y. S. Park, J. Cho, J. S. Im, C. Sone, Y. Park, W. J. Choi, and Q. H. Park, *Appl. Phys. Lett.* **87**, 203508 (2005).
- <sup>13</sup>S. H. Kim, K. D. Lee, J. Y. Kim, M. K. Kwon, and S. J. Park, *Nanotechnology* **18**, 055306 (2007).
- <sup>14</sup>J. Y. Kim, M. K. Kwon, K. S. Lee, S. J. Park, S. H. Kim, and K. D. Lee, *Appl. Phys. Lett.* **91**, 181109 (2007).
- <sup>15</sup>S. G. Johnson and J. D. Joannopoulos, *Photonic Crystal* (Kluwer, Boston, 2002).
- <sup>16</sup>M. K. Kwon, I. K. Park, J. Y. Kim, J. O. Kim, B. Kim, and S. J. Park, *IEEE Photonics Technol. Lett.* **19**, 1880 (2007).
- <sup>17</sup>M. S. Oh, M. K. Kwon, I. K. Park, S. H. Baek, S. J. Park, S. H. Lee, and J. J. Jung, *J. Cryst. Growth* **289**, 107 (2006).
- <sup>18</sup>C. C. Wang, H. Ku, C. C. Liu, K. K. Chong, C.-I. Hung, Y. H. Wang, and M. P. Houg, *Appl. Phys. Lett.* **91**, 121109 (2007).
- <sup>19</sup>S. Watanabe, N. Yamada, M. Nagashima, Y. Ueki, C. Sasaki, Y. Yamada, T. Taguchi, K. Tadatomo, H. Okagawa, and H. Kudo, *Appl. Phys. Lett.* **83**, 4906 (2003).
- <sup>20</sup>T. Mukai, K. Takekawa, and S. Nakamura, *Jpn. J. Appl. Phys., Part 2* **37**, L839 (1998).